



Mitigation of the supermode noise in a harmonically mode-locked ring fiber laser using optical injection

V. A. RIBENEK,¹ D. A. STOLIAROV,^{1,2} D. A. KOROBKO,^{1,*}  AND A. A. FOTIADI^{1,3} 

¹Ulyanovsk State University, 42 Leo Tolstoy Street, Ulyanovsk, 432017, Russia

²Aston Institute of Photonic Technologies, Aston University, Birmingham B4 7ET, UK

³Electromagnetism and Telecommunication Department, University of Mons, Mons, B-7000, Belgium

*Corresponding author: korobkotam@rambler.ru

Received 27 August 2021; revised 14 October 2021; accepted 16 October 2021; posted 21 October 2021 (Doc. ID 441630); published 15 November 2021

We report on a new, to the best of our knowledge, technique enabling mitigation of the supermode noise (and timing jitter) in a soliton harmonically mode-locked (HML) fiber laser built on the nonlinear polarization evolution (NPE). An optical injection of an external continuous wave (CW) into the HML laser cavity results in an increase of the supermode noise suppression level (SSL) by a two-three order of magnitude for harmonics between 25th and 135th. The operation mechanism involves phase-locking between the injected light and soliton pulses and exhibits strong resonant dependence on the CW laser wavelength. Our findings offer important insights into the HML laser dynamics associated with an interaction between solitons and CW background in the laser cavity. © 2021 Optical Society of America

<https://doi.org/10.1364/OL.441630>

Ultrafast laser sources delivering pulses with the pulse repetition rate (PRR) in sub-GHz and GHz range are of great interest for many applications in spectroscopy, microwave photonics, ranging sensing, and telecommunications. [1]. Mode-locked fiber lasers have become a valuable alternative to semiconductor and solid-state lasers ensuring high beam quality, simplicity in adjustment, reliability, user-friendly light output, all inherent to the laser configurations spliced in all-fiber format. Because the fundamental PRR of the mode-locked lasers is determined by the cavity length, it is limited by hundreds of MHz for the fiber lasers of standard cavity length. In the HML regime, the multiple pulses are evenly spaced inside the cavity, and the laser emits regular pulses with much higher PRR equal to an integer multiple of the fundamental PRR [2]. The HML could be implemented in the fiber laser cavity using a special intracavity periodic filter [3] or through an active mode-locking procedure [4]. However, the most attractive way is the use of the passive harmonic mode-locking mechanism exploiting the pulse repulsion in the ring laser cavity [2,5–7]. A wide range of passive HML laser configurations employing either real (e.g., SESAM, carbon nanotubes) or artificial (e.g., nonlinear polarization rotation, Kerr lens) saturable absorbers have been employed

with the HML fiber lasers providing PRR up to tens of GHz [8]. The main drawback of the HML laser technology is the noise-induced irregularities of the time interval between the delivered pulses known as the HML timing jitter. Generally, its value is much higher than that of the lasers operating fundamental mode-locking [9,10]. Therefore, physical mechanisms enabling jitter reduction in HML fiber lasers are of great practical importance [11–17]. The role of background radiation as a mediator providing the equalizing interaction between pulses has been intensively discussed in this context [18–20]. The experiments on the CW light injection in the HML laser cavity have revealed its minor effect on the laser operation, whatever its wavelength [8].

In this Letter, we study the effect of the CW light injected into the HML laser cavity from an external CW narrow-band laser source on the HML laser operation. We demonstrate that under a proper system adjustment the phase-locking between the injected CW light and optical solitons induces a shift of the soliton carrier frequency. The carrier frequency shift accelerates relaxation of the perturbed HML laser system based on the interpulse repulsion to an equilibrium state thereby ensuring an advanced equalization of the pulse arrangement inside the cavity [10,21,22]. The HML laser supermode noise is evaluated through the supermode suppression level (SSL) measured in laser RF spectrum. The effect exhibits a strong resonant dependence on the injected CW light wavelength and makes no impact on other laser performance characteristics. In particular, we demonstrate a reduction of the supermode noise by two–three orders of magnitude in the HML laser configuration based on a 15.5-m-long ring cavity enabling pulses with the PRR adjustable in the range of 350 MHz–1.88 GHz.

The experimental configuration of an Er-doped soliton NPE mode-locked fiber ring laser is shown in Fig. 1. The laser cavity consists of two types of fibers: 0.8 m length of heavily erbium-doped fiber (EDF) with normal dispersion (−48 ps/nm/km) and standard single mode fiber (SMF-28) with anomalous dispersion (17 ps/nm/km). The total length of the laser cavity of 15.5 m corresponds to the fundamental PRR $f_0 = 14.1$ MHz. Polarization-dependent fiber isolator (PD ISO), two 980/1550

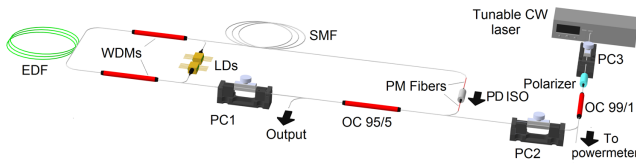


Fig. 1. Experimental HML laser setup.

WDM couplers, in-line polarization controller (PC1) and 5% output coupler (OC) are incorporated into the cavity. The laser is pumped at 980 nm from two laser diodes specified for maximum power of 550 mW.

The central wavelength of the soliton laser operation can be selected by a rough polarization controller (PC1) adjustment from a few spectral bands from 1550–1590 nm specific for the built fiber configuration.

The light from the external tunable PM laser source “Yenista T100” is used for injection into the HML laser cavity. The CW laser is tunable in the range of 1550–1590 nm and set to operate with the linewidth of ~ 100 kHz and output power of ~ 3.5 mW. PC2 and PC3 are used for independent control of the injected CW light polarization state and power, respectively. With the built laser configuration, PC2 is adjusted once for maximal transparency of the HML fiber cavity to the injected light and then PC2 settings are fixed. The injected CW light power smoothly controlled by PC3 is monitored by the power meter (Fig. 1). Evidently, direct CW laser power tuning by buttons on the CW laser panel allows removal of PC3. However, in our case, power control with PC3 is more practical, since the laser may exhibit wavelength and linewidth variations when its power level is changed. The HML laser operation is monitored by an optical spectrum analyzer (HP 70950B) with resolution of 0.1 nm and RF spectrum analyzer (R&S FSP40) coupled with a 30 GHz photodetector (MACOM D-8IR).

Figure 2 highlights details of the laser operation without and with optical injection. Controls of the HML laser pump power and PC1 only are used to adjust the laser operation regime. With a rough PC1 adjustment, the laser wavelength is set to $\lambda \sim 1558$ nm. Without optical injection, the laser operation is typical for HML lasers based on the NPE mechanism. Once the lasing threshold (30 mW) is achieved, the mode-locking regime is established. At a low pump power level (~ 80 mW), the laser still emits regular pulses with the fundamental PRR $f_0 = 14.1$ MHz. In this regime, only a single soliton pulse circulates inside the laser cavity. With an increase of the pump power, the laser switches to multipulse operation. A delicate adjustment of PC1 at this stage equalizes distribution of the generated pulses inside the cavity thus enabling HML. In the HML regime, the laser emits regular pulses with the PRR equal to N pulses per cavity round trip, $f_{\text{rep}} = Nf_0$. The PRR could be increased by an increase of pump power. Besides, at each pump power level the PRR could be also tuned by fine adjustment of PC1. Figures 2(a)–2(e) (red lines) show the optical and RF HML laser spectra recorded at the fixed total pump power of 700 mW (both laser diodes contribute equally) and different PRR. Precise adjustment of PC1 has a minor effect on the laser central wavelength and output power, but allows the PRR change over the range of 0.3–3.5 GHz. With the PRR increase, the laser output power just slightly increases from 3.45 (at 300 MHz) to 3.48 mW (at 3.5 GHz), but the laser energy accounted for a single soliton decreases significantly from 6.7 down to 1.5 pJ, respectively. The laser pulse widths have been measured as ~ 0.5 ps (at ~ 517 MHz) and ~ 2.2 ps (at 2.28 GHz). The narrower soliton pulses at a lower PRR possess broader optical spectra shown in Fig. 2. The broader optical spectra exhibit pronounced Kelly sidebands. Their amplitude rapidly decreases as the soliton spectrum becomes narrower with the PRR increase. PRR tuning could be monitored with the RF spectrum analyzer. A typical RF spectrum of the HML laser consists of the main

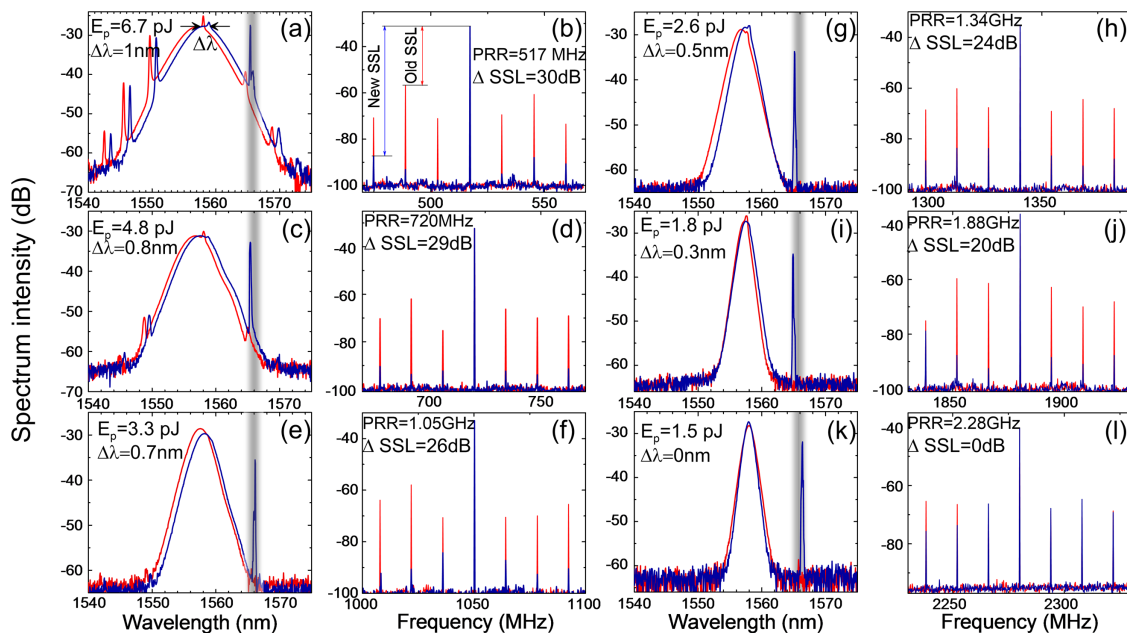


Fig. 2. Optical and RF spectra recorded with the HML fiber laser before (red curve) and after (blue curve) the CW light injection at different PRR. The single soliton energy E_p , optical spectrum shift $\Delta\lambda$, SSL difference before and after the CW injection ΔSSL , PRR are also depicted. RF spectra have been obtained in a 100 MHz span with a 200 kHz resolution. The only FTM band in the presented spectrum range is marked (grey).

peaks and small peaks surrounding them. The main peaks are spaced by the PRR, whereas the surrounding small peaks are spaced by the fundamental PRR, f_0 . A ratio between the main peak amplitude and the maximal amplitude of the surrounding supermodes is referred to as the supermode noise suppression level (SSL) that is the key HML laser parameter characterizing the periodicity of pulse emission (the timing jitter) [8]. One sees that the SSL of ~ 20 dB is nearly the same for the HML laser operating with the PRR in the range of 0.5–3.5 GHz.

In the HML laser dynamics based on the NPE mechanism, the fiber birefringence filter plays a crucial role. The spectral transmittance peaks of the filter are spaced periodically, and for the considered laser implementation are centered around the wavelengths $\lambda \sim 1544, 1555, 1566,$ and 1577 nm. Narrow (<1 nm) bands centered at these wavelengths are referred hereinafter to as the filter transmittance maximum (FTM) bands (one of them is marked in Fig. 2). The result of CW light interaction with the HML laser radiation inside the cavity depends on: (1) the position of the HML laser optical spectrum in respect to FTM bands, (2) the wavelength, (3) power, and (4) polarization state of the injected light, all adjusted independently by PC1, the wavelength control buttons on the CW laser panel, PC3 and PC2, respectively (see Supplement 1 for the detailed setup adjustment). The mandatory condition for the effects reported in this Letter is that the Kelly sideband of the HML laser optical spectrum has to be within one of the FTM bands (see, Fig. 2). The HML laser optical spectrum always could be shifted to the required position using rough PC1 adjustment. At the same time, fine adjustment of PC1 has a minor effect on the spectrum position but allows to change the PRR as shown in Fig. 2. The birefringence filter transmittance determines also the injected CW light power circulating inside the HML laser cavity. Selection of the CW laser wavelength within the FTM bands maximizes the injected CW light power. PC2 settings are fixed ensuring the maximal transparency of the HML fiber cavity to the injected light. To highlight the effect of the CW light injection on the HML laser operation, one scans the CW laser wavelength over the optical spectrum using the buttons on the CW laser panel. Until the CW laser wavelength is far from the HML laser wavelength, no modification of the HML laser spectra occurs. On the contrary, a close approach of the CW laser line to the HML laser wavelength stops the HML laser operation destroying regular pulsations. However, the most curious effects are observed when the CW light line approaches (or is directly injected into) the Kelly sideband properly fixed within the FTM band in advance. In other words, the double coincidence of the injected CW light wavelength with the Kelly sideband and with FTM band is the necessary condition for the effects reported in this Letter.

For the HML laser operation shown in Fig. 2, the HML laser wavelength is set near $\lambda \sim 1558$ nm, and the nearest Kelly sideband is within the FTM band centered at $\lambda \sim 1566$ nm. The injected CW light power is ~ 3.5 mW. With the CW light injection beyond this FTM band, no effect on the HML laser behavior is observed. However, the CW light injected into the same FTM band may have an effect. Figures 2(a) and 2(b) show the optical and RF spectra of the HML laser operating with the PRR of 570 MHz. One sees that the supermode noise level in the RF spectrum drops down when the CW light wavelength is injected into the Kelly sideband. The SSL increases from 25 (before the CW injection) to 55 dB (after the CW injection),

i.e., by three orders of magnitude (30 dB). Importantly, once the CW is injected, the top of the optical spectrum is shifted by $\Delta\lambda \approx 1$ nm towards the CW line (see, Visualization 1). Direct measurements of the pulse timing jitter highlight its reduction from ~ 8.2 to ~ 1.85 ps. We have found that the induced effects possess a threshold dependence on the injected CW light power. A gradual decrease of the injected power reduces simultaneously the SSL and induced frequency shift. At the CW power of ~ 0.5 mW (and lower), the SSL gets its original value of 25 dB, and no frequency shift occurs.

The same effect is observed at higher PRR as well [Figs. 2(c)–2(j)]. Surprisingly, it is still observed even at PRR > 800 MHz, when the Kelly sideband is no longer registered by the spectrum analyzer. Although the Kelly sideband amplitude decreases with the PRR, its position within the optical spectrum remains nearly fixed [23]. Therefore, using PC1 this spectral point could be fixed within the FTM band resulting in the supermode noise reduction induced by the CW light injected into the same spectral point [see Figs. 2(c)–2(j)]. One sees that with the PRR increase the reported effect becomes less pronounced. For the HML laser operating at 1.88 GHz, the CW light injection still reduces the supermode noise by 20 dB. This noise reduction is accompanied by a shift of optical spectrum towards the CW line by $\Delta\lambda \approx 0.3$ nm. With higher PRR > 2 GHz, i.e., at soliton energies $E_p < 1.7$, no significant effect of the CW light injection on the HML laser noise properties is observed.

The resonant CW light injection reduces the supermode noise in rather a wide RF spectrum range. Figure 3 shows the RF spectra recorded with the HML laser operating at 517 MHz and 1.88 GHz without and with the resonant CW light injection. Specifically, the RF spectra are recorded in an extended spectrum range covering several harmonics. In both cases, the injection of resonant CW light into the HML laser cavity reduces the noise RF spectrum background extended over >7 GHz by ~ 20 dB thus improving the laser performance, including the timing jitter.

All described effects are observable with any FTM band once it coincides with the CW light wavelength and Kelly sidebands of different orders (see Supplement 1).

Although the detailed theoretical description of the laser operation is in progress, we believe there is no contradiction between the reported observations and current understanding

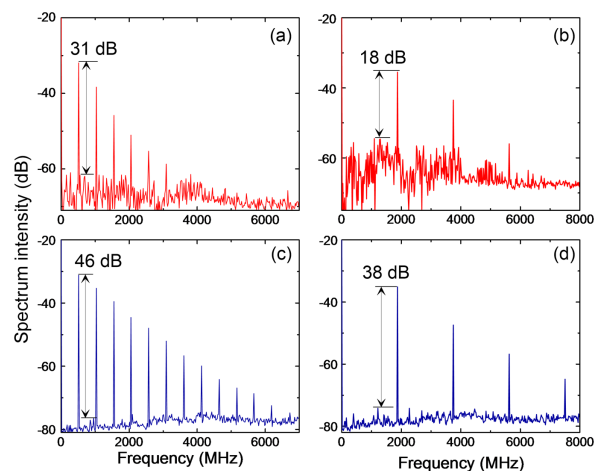


Fig. 3. RF HML laser spectra recorded with a resolution bandwidth of 20 MHz (a), (b) before and (c), (d) after the CW injection at PRR (a), (c) 517 MHz, (b), (d) 1880 MHz.

of the mechanisms underlying the equalization of multi-pulse distribution inside the fiber cavity [10,22]. The effect is observed only with the CW light wavelength approaching the Kelly sideband in the laser optical spectrum. The Kelly sidebands originate from the phase-locking between the solitons and dispersive wave when for some optical frequencies their relative phase changes by an integer multiple of 2π per cavity round trip. In this context, we believe that the injection of a narrow-band CW light at the frequency of the Kelly sideband into the HML laser cavity seeds the wave strongly phase-locked with the solitons. In this state, the injected CW light enables control of the soliton propagation affecting the soliton carrier frequency [24]. As a result, the CW light injection induces the soliton carrier frequency shift as it is observed in the experiment.

The frequency shift of the soliton carrier frequency plays a crucial role in the supermode noise suppression. In the HML lasers based on pulse repulsion, the carrier frequency shift accelerates evolution of the perturbed system to the equilibrium state with equidistant distribution of the pulses inside the cavity (that is equivalent to the enhanced interpulse repulsion [22]) reducing the supermode noise. This understanding is in good agreement with our experimental observations. First, it accounts for the strong resonant nature of the effect. The injected light wavelength should be the same as that of the resonant dispersive wave responsible for the Kelly sideband. Second, the strong coupling between the solitons and the injected CW wave results in the frequency shift of the soliton carrier frequency. It is experimentally confirmed that the ability of the injected light to reduce the supermode noise is directly connected with the soliton carrier frequency shift induced by the CW light injection. When the soliton energy decreases (at high PRR), the interaction between the soliton and the injected light becomes weaker. It leads to the smaller soliton carrier frequency shift and, hence, lower suppression of the supermode noise. The same speculations are applicable to the effect observed with the CW light injected at the wavelengths of the second- and third-order Kelly sideband. These sidebands are always lower than the first Kelly sideband; therefore, the CW light injection at these wavelengths causes the smaller soliton carrier frequency shift and, hence, provides the weaker supermode noise suppression.

In conclusion, we have offered the method of supermode noise suppression in the soliton HML fiber laser built on NPE. The method employs a direct injection of narrow-band CW light from an external laser source into the HML laser cavity. To demonstrate these phenomena, we have experimentally studied the soliton laser configuration comprising the 15-m-long ring fiber cavity and achieved an increase of the SSL by two–three orders of magnitude at PRR ranging from 350 MHz–1.88 GHz. Although our experimental setup is similar to that used earlier (e.g., [8]), the mandatory conditions for the noise mitigation effect, i.e., coincidence of the Kelly sideband with an FTM band, have not been satisfied in the previous works. Under this condition, the effect exhibits a strong resonant dependence on the CW laser wavelength and is available at the wavelengths near the Kelly sidebands of the HML laser spectrum ensuring phase-locking between the CW and solitons. The soliton frequency shift arising due to phase-locking leads to the accelerated evolution of the system to the equilibrium point equalizing arrangement of pulses in the HML laser cavity. The direct connection between the supermode noise suppression effect, soliton carrier frequency shift, and soliton energy is explored. The effect

has been observed with the CW light wavelength near the Kelly sidebands of different orders (up to the third order), but with the second- and third-order Kelly sidebands the effect is less pronounced. We believe that our findings offer important insights into the HML laser dynamics associated with the interaction between background radiation and solitons that is crucial for the HML laser design and optimization. The proposed technique can be used to reduce the timing jitter of the HML fiber laser down to the level of lasers operating fundamental mode-locking, thus making the HML lasers promising for an extended range of applications.

Funding. Russian Science Foundation (19-72-10037); Ministry of Science and Higher Education of the Russian Federation (075-15-2021-581).

Disclosures. The authors declare no conflicts of interest.

Data Availability. Data underlying the results presented in this Letter are not publicly available at this time but may be obtained from the authors upon reasonable request.

Supplemental document. See Supplement 1 for supporting content.

REFERENCES

1. S. A. Diddams, K. Vahala, and T. Udem, *Science* **369**, 6501 (2020).
2. X. Liu and M. Pang, *Laser Photon. Rev.* **13**, 1800333 (2019).
3. D. A. Korobko, A. A. Fotiadi, and I. O. Zolotovskii, *Opt. Express* **25**, 21180 (2017).
4. Y. Wang, S. Y. Set, and S. Yamashita, *APL Photon.* **1**, 071303 (2016).
5. H. Cheng, W. Wang, Y. Zhou, T. Qiao, W. Lin, Y. Guo, and Z. Yang, *Opt. Express* **26**, 16411 (2018).
6. J. N. Kutz, B. C. Collings, K. Bergman, and W. H. Knox, *IEEE J. Quantum Electron.* **34**, 1749 (1998).
7. H. J. Khashi, S. V. Sergeev, M. Al-Arjami, A. Rozhin, D. Korobko, and A. Fotiadi, *Opt. Lett.* **44**, 5112 (2019).
8. C. Lecaplain and P. Grelu, *Opt. Express* **21**, 10897 (2013).
9. F. Rana, H. L. Lee, R. J. Ram, M. E. Grein, L. A. Jiang, E. P. Ippen, and H. A. Haus, *J. Opt. Soc. Am. B* **19**, 2609 (2002).
10. R. V. Gumenyuk, D. A. Korobko, and I. O. Zolotovskii, *Opt. Lett.* **45**, 184 (2020).
11. M. Nakazawa, K. Tamura, and E. Yoshida, *Electron. Lett.* **32**, 461 (1996).
12. O. Pottiez, O. Deparis, R. Kiyon, M. Haelterman, P. Emplit, P. Mégret, and M. Blondel, *IEEE J. Quantum Electron.* **38**, 252 (2002).
13. J. Schröder, D. Alasia, T. Sylvestre, and S. Coen, *J. Opt. Soc. Am. B* **25**, 1178 (2008).
14. L. Yuhua, L. Caiyun, W. Jian, W. Boyu, and G. Yizhi, *IEEE Photon. Technol. Lett.* **10**, 1250 (1998).
15. G.-R. Lin, M.-C. Wu, and Y.-C. Chang, *Opt. Lett.* **30**, 1834 (2005).
16. X. Shan and D. M. Spirit, *Electron. Lett.* **29**, 979 (1993).
17. D. Zhao, Y. Lai, X. Shu, L. Zhang, and I. Bennion, *Appl. Phys. Lett.* **81**, 4520 (2002).
18. G. Semaan, A. Komarov, M. Salhi, and F. Sanchez, *Opt. Commun.* **387**, 65 (2017).
19. E. Averlant, M. Tlidi, K. Panajotov, and L. Weicker, *Opt. Lett.* **42**, 2750 (2017).
20. B. Kostet, S. Gopalakrishnan, E. Averlant, Y. Soupart, K. Panajotov, and M. Tlidi, *OSA Contin.* **4**, 1564 (2021).
21. D. A. Korobko, D. A. Stoliarov, P. A. Itrin, M. A. Odnoblyudov, A. B. Petrov, and R. V. Gumenyuk, *J. Lightwave Technol.* **39**, 2980 (2021).
22. D. A. Korobko, D. A. Stoliarov, P. A. Itrin, M. A. Odnoblyudov, A. B. Petrov, and R. V. Gumenyuk, *Opt. Laser Technol.* **133**, 106526 (2021).
23. M. L. Dennis and I. N. Duling, *IEEE J. Quantum Electron.* **30**, 1469 (1994).
24. A. Komarov, H. Leblond, and F. Sanchez, *Phys. Rev. A* **71**, 053809 (2005).